Mapping Land Cover Types in Amazon Basin Using 1km JERS-1 Mosaic

Sassan S. Saatchi[1], Bruce Nelson[2], Erika Podest[1], John Holt[1]

1. Jet Propulsion Laboratory
California Institute of Technology
4800 Oak Grove Drive
Pasadena, California 91109

2. Instituto Nacional de Pesquisas de Amazonia
CP 478, Ecologia
69011-970, Manaus
Amazonia, Brazil

Abstract

During the Global Rain Forest Mapping (GRFM) project, JERS-1 SAR (Synthetic Aperture Radar) satellite was used to map the humid tropical forests of the world. The rationale for the project was to demonstrate the application of the spaceborne L-band radar in tropical forest studies. In particular, the use of data for mapping land cover types, estimating the area of floodplains, and monitoring deforestation and forest regeneration were of primary importance. In this paper, we examine the information content of the JERS-1 SAR data for mapping land cover types in the Amazon basin. More than 1500 high resolution (12.5 m pixel spacing) images during the low flood period of the Amazon river were mosaicked to a seamless 100 m resolution image over the entire basin, covering an area of about 8 million km^2. This image was used in a classifier to generate a 1 km resolution land cover map. The inputs to the classifier were 1km resolution mean backscatter and seven first order texture measures derived from the 100 m data by using a 10 x 10 independent sampling window. The classification approach included two interdependent stages: 1) a supervised maximum *a posteriori* Baysian approach to classify the mean backscatter image into 5 general land cover categories of forest, savanna, swamp, white sand, and anthropogenic vegetation classes, and 2) a texture measure decision rule approach to further discriminate subcategory classes based on taxonomic information and biomass levels.

The general category and the subcategory classes were identified from the RADAMBRASIL Project 1: 1,000,000 vegetation map and several field studies. For each class 10 sites were chosen for training and validation of the classifier. After several iterations and combining land cover maps, 14 classes were successfully separated at 1km scale. The results were verified by examining the accuracy of the approach using the validation test sites, and comparison with the RADAM and the AVHRR based 1 km resolution land cover maps.

1. Introduction

In recent years, several interdisciplinary studies within the international scientific communities have focused on understanding the processes of land cover and land use change in the tropical rainforests and the subsequent effects on the earth atmosphere. Tropical forests, because of the large area of land surface they cover (about 1600 million hectares at the climatic climax), their humid climate (rainfall of above 2000 mm per year), and being the most luxuriant and species-rich forests, are responsible for the major proportion of the earth's biological productivity. A large part of the tropical rainforests in the world is undergoing extensive land transformation as a result of population growth and economic development and pressures. Such changes directly influence the processes that govern the interaction of land surface with the atmosphere. This represents, for example, changes in a vast intake of the CO_2 which is stored in the tree tissue and thus the carbon cycling, changes in the hydrological processes and their influence in fluxes of water and trace gasses, the geomorphology of river basins, and changes in biodiversity and habitat of endemic species (Myers, 1988; Myers, 1992; Houghton, 1995).

Understanding the human or climate induced changes of tropical landscape requires a basic knowledge of the current status of the ecosystem, the area and the type of the land cover susceptible to changes, and the causes and impacts of these changes. Recent advances in remote sensing technologies have partially contributed in documenting and monitoring these changes (INPE, 1992; Skole and Tucker, 1993). However, there are several unresolved problems associated with mapping the land cover types and monitoring the tropics on regional and continental scales. These problems are primarily associated with the limitation of current remote sensing techniques and the methodologies used in both defining the land cover types and identifying the parameters to be monitored.

Optical remote sensing has been used for classification of land cover types and the study of changes on local to regional scale. High resolution (30 m) Landsat Thematic Mapper (TM) data has been the primary source for estimating the rate of deforestation by INPE (Instituto Nacional de Pesquisas Espaciais) and Landsat Pathfinder Program (INPE, 1992; Skole and Tucker, 1993; Justice and Thownshend, 1994). These studies have used visual interpretation and classification as their primary approach for extracting thematic information. Most large scale maps derived from these studies have limited land cover

types. This is primarily due to difficulties in interpreting the spectral information in Landsat data acquired at different years or seasons.

Coarse resolution (1.1 km) NOAA AVHRR (Advanced Very High Resolution Radiometer) provides global observation at high temporal sampling and can be used for large scale mapping and monitoring (Tucker et al., 1985; Stone et al., 1994; Thownshend and Justice, 1988; DeFries and Thownshend, 1994). The AVHRR data have been used in different ways. Among them the multitemporal derived NDVI (Normalized Difference Vegetation Index) from Global Area Coverage (GAC) data is the most reliable data set for land cover classification. The classification of this data set has been performed on a global scale and thus with limited classes over the tropical region (DeFries and Thownshend, 1994; DeFries et al., 1998). In addition, few continental scale products have been produced from GAC data over South America and Africa (Thownshend et al., 1987; Tucker et al., 1985; Malingreau et al., 1995) respectively. Recently, a combination of AVHRR LAC (Local Area Coverage) at 1 km and the AVHRR GVI (Global Vegetation Index) data at 15-25 km resolution have been used to produce a more detailed vegetation map of South America (Stone et al., 1994).

Microwave sensors, such as radar, in large, have remained unexploited. The reasons are varied, and at times controversial, depending on the application. Nevertheless, the reasons can be found in: 1) lack of long term availability of data from spaceborne or airborne radar systems over a large area of tropical forests, 2) lack of appropriate bands and polarization channels on current spaceborne systems, 3) the difficulty in interpreting radar backscatter data as compared to photo or optical spectral characteristics, and 4) the tradition in geography and earth science disciplines for the use of optical remote sensing data versus military and engineering community for the use of radar data.

During the past decade, several radar sensors have been deployed in space such as the shuttle imaging radar (SIR-A, SIR-B, and SIR-C/X-SAR), ERS-1,2, JERS-1, and Radarsat. Except the SIR-C/X-SAR system, all radar sensors have only one channel. Though none were designed specifically for land cover mapping, several investigations have demonstrated that the data provides unique information about the characteristics of the tropical landscapes (Sader, 1987; Foody and Curran, 1994). First, the radar data can be acquired as frequently as possible due to insensitivity to atmospheric condition and sun angle. This will allow continental scale high resolution data for systematic assessment of deforestation and regrowth processes. Second, depending on the wavelength, the radar backscatter signal carries information about the forest structure and moisture condition by penetrating into the forest canopy. Few studies have addressed these characteristics by

3

using the radar data for mapping tropical land cover and estimating the biomass of regenerating forests (Foody and Curran 1994; Luckman et al., 1997; Saatchi et al., 1997; Rignot et al., 1997).

In this paper, we demonstrate the use of the JERS-1 SAR data for mapping land cover types over the Amazon basin. The JERS-1 data were acquired during the GRFM (Global Rain Forest Mapping) project in 1995 and 1996 in order to assess the use of the data for mapping and monitoring tropical landscape. To make the results compatible with the ongoing large scale mapping projects with optical sensors, we created a one kilometer resolution JERS-1 mosaic derived from resampling higher resolution images (12.5 m pixel spacing). In section 1, we discuss the data acquisition and properties during the GRFM project. In section 2, we develop a supervised two stage classification approach based on the backscatter and texture measures and a training data set extracted from images over several land cover types. After determining the types of land covers that can be classified with the 1km mosaic data, we employ the classifier to discriminate the landscape classes in the image mosaic. The resulting map is compared with the RADAM Brazil derived map and the 1 km AVHRR classification (Hansen et al., 1998). These data sets and the ground information from several studies are used to determine the accuracy of the JERS-1 classification.

2. JERS-1 SAR Observation

JERS-1 SAR is an L-band spaceborne SAR system launched by the National Space Development Agency of Japan (NASDA) in February, 1992. The system operates at 1.275 GHz with horizontal polarization for both transmission and reception. The spatial resolution of the system is 18 m in both azimuth and range. The swath width is 75 km and the incidence angle of radar at the center of swath is 38.5°. The single-look images have 4.2 m pixel spacing in azimuth and 12.5 m in range and the standard three look image data has 12.5 m pixel spacing in both azimuth and range. JERS-1 covers the global land surface for several applications such as land survey, agriculture, forestry, fishery, environmental protection, disaster prevention and coastal monitoring. The satellite flies on sun synchronous orbits 568 km above the Earth surface and with a recurrent period of 44 days. In late 1995, JERS-1 satellite entered into its Global Rain Forest Mapping (GRFM) phase and has been collecting high resolution SAR data over the entire tropical rainforest. In a short period (approximately 60 days), during the GRFM phase, the satellite provided

continental scale data over tropics. Because of cloud cover, similar coverage with high resolution optical data such as Landsat can only be provided on annual or decadal time frame (Justice et al., 1997). The JERS-1 coverage of the Amazon basin is shown in Figure 1.

3. Image Mosaic

One of the main problems in using high resolution imagery to provide regional or continental scale maps is the difficulty of mosaicking a large number of images. This is due to inaccurate orbital information, changes in surface feature between two adjacent data takes, and calibration discrepancies among images. In optical imagery, to these problems, one can add the changes of sun angle for each data take, the lack of frequent data takes in one season, and thus spectral changes of landscape. In the case of JERS-1 images over the Amazon basin, these problems can be readily overcome because 1) all images are taken in two months minimizing changes in surface features, 2) JERS-1 data can be cross calibrated to provide uniform calibration over the entire mosaic, and 3) the atmospheric condition does not affect the image quality.

In this study, we have used 100 m resolution JERS-1 data (8 by 8 averaging of high resolution data) to generate a map of the entire basin from 1500 images. The details of mosaicking technique is given in Siqueira et al., (1998). The technique has been developed on the foundation of a mathematical approach to mimic a wallpapering approach by minimizing the propagation of errors. The interscene overlap both in the along-track and cross-track directions are used for individual scene geolocation. The scenes are placed on a global coordinate system with the flexibility of having scenes floating freely with respect one another until the locations of all scenes are calculated simultaneously avoiding any directional errors. The result is an optimum seamless mosaic. The geometrical accuracy of the mosaic is performed by choosing forty one control points from a Brazilian and Peruvian 1:100,000 scale maps. It is found that 95% of the control points can be located within one pixel (100 m) or less. The final mosaic is projected in an equal area projection which resulted in resampling of the image to 3 arc second pixel size (approximately 90 meter). Note that unlike the high resolution raw images, after averaging and resampling the pixel spacing and the ground resolution of the final mosaic image are approximately equal (Figure 2).

4. Classification Methodology

The coherent nature of the radar backscatter signal suggests that the imaging radar data contains two components: one is the speckle which is due to the scattering from randomly distributed scatterers in a pixel, the other is the texture resulting from the spatial variability of the scene illuminated by the radar. The speckle often causes uncertainty in interpreting the radar data but the texture helps identifying scene characteristics in images. There are several filtering techniques to reduce the speckle in SAR data and meanwhile to preserve the texture information. The discussion on these techniques is outside the scope of this paper (see e.g. Ulaby et al., 1986). We start our analysis based on the *a priori* knowledge that textural information enhances the capability of per-pixel basis classification of SAR data. Textural information or measures are extracted from different order image histograms by using various degrees of signal statistics (Ulaby et al., 1986; Posner, 1993; Anys and He, 1995; Soares et al., 1996).

In classifying the JERS-1 SAR data, we develop texture measures based on the first order histogram derived in *a priori* specified window size. These measures characterize the frequency of occurrence of the grey level within the window in the single channel radar data and they depend on the size of the window. In this study, we develop the texture measures from the 100 m JERS-1 mosaic over a 10 x 10 window in order to produce 1 km images. The window is moved blockwise in the image, reducing the resolution and catching the signal statistics up to the scale of the window size (i.e. one kilometer).

We understand that the choice of a large window for transforming 100 m resolution images to 1 km may reduce the accuracy of land cover mapping by introducing mixed information in large pixels and errors in the definition of edges of land parcels. The resulting texture images have independent pixel information, and are reduced in size by a factor of 10 in each dimension. Note that the JERS-1 SAR image is treated as a grey level image as in any type of imagery. However in interpreting the tonal and texture variations in the image we use the general characteristics of SAR data such as the penetration in the vegetation canopy, and sensitivity to structure and moisture condition.

4.1. Texture Measures

In quantifying the texture measures, we use the amplitude mosaic image. The use of amplitude instead of intensity helps separating low vegetation and water classes because of the small dynamic range of JERS-1 data (approximately 18 dB) and low signal to noise ratio. Local texture measures derived from the first order histogram of a 10 x 10 window are given as follows:

6

1) Mean $(S_M) = \sum_{i=0}^{k-1} iP(i)$ (1)

where $P(i) = N(i)/M$, $N(i)$ is number of pixels of same grey level in window, i is the pixel grey level, and k is the maximum possible grey level.

2) Variance $(S_D^2) = \sum_{i=0}^{k-1} (i - S_M)^2 P(i)$ (2)

The variance characterizes the way in which values are distributed around the mean. It is basically a measure of heterogeneity. Variance measure increases when there is much difference on gray level values from their mean

3) Entropy $= -\sum_{i=0}^{k-1} P(i) \ln[P(i)]$ (3)

Entropy is a measure of the amount of disorder in an image. The greater the noise on the image, the higher the entropy values are.

4) Energy $= \sum_{i=0}^{k-1} [P(i)]^2$ (4)

Energy is a measure of the homogeneity of the image (only similar grey levels are present). It can be regarded as the opposite of entropy. When all the grey level pixels within a window are constant then the energy is one.

5) Contrast $= \sum_{i=0}^{k-1} (i_{max} - i_{min})^2 P(i)$ (5)

Contrast is the difference between the highest and lowest values in the window and it increases by local variations of grey level.

6) Skewness $= \frac{1}{S_D^3} \left[\sum_{i=0}^{k-1} (i - S_M)^3 P(i) \right]$ (6)

Skewness characterizes the degree of asymmetry of the distribution of pixel values around the mean.

7) Kurtosis $= \frac{1}{S_D^4} \left[\sum_{i=0}^{k-1} (i - S_M)^4 P(i) - 3 \right]$ (7)

Kurtosis is a measurement of the relative peakedness or flatness of the pixel distribution.

7

4.2. Texture Measure Selection

Texture measures calculated for classification are from the first order histogram, they are correlated and do not contribute equally to discriminating classes. In order to evaluate the properties of textures and their effectiveness in separating classes, we use a figure of merit approach. In this approach, we establish a distance between the classes of the image from a training data set in such a way that a large distance implies a better class separability and thus small classification error. The distance is a statistical difference between the probability density functions of two classes i and j, and are often called the B distance (Bhattacharyya distance) or Jeffries-Matusia distance (Swain and King, 1973). Assuming that the probability density functions have Gaussian distribution, the B distance can be calculated as follows:

$$B = 2(1 - e^{-\rho}) \tag{9}$$

where:

$$\rho = \frac{1}{8}(\mu_1 - \mu_2)^{\mathrm{T}} \left[\frac{\Sigma_1 + \Sigma_2}{2}\right]^{-1} (\mu_1 - \mu_2) + \frac{1}{2} \ln \left[\frac{\left|\frac{1}{2}(\Sigma_1 + \Sigma_2)\right|}{|\Sigma_1|^{\frac{1}{2}}|\Sigma_2|^{\frac{1}{2}}}\right] \tag{10}$$

with: μ_1: mean vector for class 1 (dimensions=nx1, where n is the number of classes)

Σ_1: covariance matrix of class 1 (dimension=nxn)

$|\Sigma_1|$: determinant of Σ_1

The exponential factor gives an exponentially decreasing weight to increasing separations between textural classes.

Since $0 \leq e^{-\rho} \leq 1$ then the B-distance varies between 0 and 2, with two corresponding to the maximum separability between classes. This distance is also directly related to the classification error probability in case of a Baysian classifier which assumes a Gausian

distribution. The rate of correct classification, P_c, of B-distance is situated between (Swain, 1978):

$$1 - \left(\frac{1}{4}(2 - B_{1,2}) \right) \leq P_c \leq \left(1 - \frac{1}{16}(2 - B_{1,2})^2 \right) \qquad (11)$$

In the following section, the texture measures from training areas within the image are extracted and by using the B distance their relative contributions for separating various classes in each land cover category are discussed. By removing less effective textures for the identification of each class, one can use a smaller set of input parameters in the classifier.

4.3 Classifier

After choosing a list of texture measures, we employ a two stage approach to perform a supervised classification of the JERS-1 mosaic. In the first stage, we use a maximum *a posteriori* Baysian (MAP) classifier on the JERS-1 mean backscatter image at 1 km scale for general categories of land cover types. The classifier is an extension of maximum likelihood Baysian classifier (MLE). The detailed description of the classifier can be found elsewhere (Rignot and Chellappa, 1993; Saatchi and Rignot, 1996). This classifier was originally developed for polarimetric SAR data. In our analysis, we have modified the classifier in order to accommodate single channel JERS-1 data. The JERS-1 SAR amplitude data are assumed to have a Gaussian distribution. From modeling the *a priori* distributions of data and image classes, a model for the *a posteriori* distributions of image classes are derived using the Bayes theorem. In other words, the MAP classifier views the classes as random variables with some *a priori* distributions and then revises the decision through an iterative procedure to optimize the decision about the nature of classes.

In the second stage, the texture measures and the MAP classified image will be used in a hierarchical decision rule based algorithm to further discriminate the classes within each general land cover category. The decision rules are derived by using predictor variables obtained from the multi-dimensional separability analysis of the backscatter and texture measures for each class type.

The learning procedure for the classifier at both stages is supervised. The training data are extracted with the *a priori* knowledge of the scene and the land cover types as shown in the RADAM map. The data from the training set will be used both for the separability test of class types in each land cover category and as supervised data set for the classifier. In the following section, we first test the separability by using the B distance and then classify the image and analyze the accuracy of the results.

Note that the input texture images to the classifier and the training data sets are

9

derived from the 100 m JERS-1 using a 10 x 10 window. The use of 100 m backscatter image rather than the 1 km images for collecting the training data, helps avoiding mixed pixel information in training data set.

5. Land Cover Types

The Amazon basin occupies a vast area of South America, nearly 6,000,000 km2, with more than half of it in the Brazilian territory. The region is a physiographic and biological entity which consists of large areas of dense forest with high biomass. The interior of this region includes small or relatively large nonforest, or forests with local variations in vegetation and floristic composition. By vegetation types of the Amazon basin, we often refer to physiognomic or landscape patterns which are practically differentiated and named by scientists and local people. In any land cover classification exercise, the main objective is to develop techniques in order to map as many landscape patterns and cover types as possible.

Four general categories of land cover types were chosen for classification of JERS-1 data. Within each general category, several types of landscapes are described and the sensitivity of the radar backscatter and texture features to each are discussed. In order to establish a uniform and consistent definition of land cover types and vegetation structure in the Amazon basin, we have consulted many sources (Prance, 1979, Pires and Prance, 1981; Sioli, 1984; Richards, 1952). However, we have chosen the classification of RADAMBRASIL as a guideline to develop training areas and compare our classification result. This will help to avoid any diversity in definition that may exist in the literature and at the same time avoids lengthy description of the vegetation types which falls outside the scope of this paper.

The vegetation classification of the RADAMBRASIL project is followed here, as presented in Veloso et al. (1991), excluding those vegetation types not found in Amazonia. (we refer to this map as RADAM throughout the paper). Though other vegetation classification systems are found for the Amazon in the literature (e.g., Pires and Prance, 1981; Prance, 1979), this system was chosen as it forms the basis of the most extensive, detailed and up-to-date vegetation mapping effort of the Brazilian Amazon (Brazil, 1972-1982). In addition, the cover types can be transformed or merged to generate any international land cover classification legends such as IGBP (International Geosphere Biosphere Program).

The RADAM map layers have recently been incorporated into an easily manipulated geographic information system available on CD-ROM (IBGE, 1997), which facilitates

comparison with the wall-to-wall L-band SAR coverage. The RADAM maps for each region of Brazil were originally published at 1:1,000,000, however, they were digitized from hard copy maps to a scale of 1:2,500,000 and incorporated in a GIS (Geographical Information System). Because of this, some features such as smaller rivers that are visible even on 1 km JERS-1 images are not seen in the IBGE (Instituto Brasileiro de Geographia e Estatistica) GIS based maps. For this study, the reference vegetation map of the Brazilian Amazon basin is derived by combining the vectors of the land cover data of RADAMBRASIL project as shown in figure 3. Table 1 describes the legend of the map and the cover types used in this study.

The map in figure 3 is organized into five hierarchical levels. The user builds a vegetation description using the Boolean operator "or" when combining vegetation descriptors available within a level, Boolean "and" for descriptors in different levels. Any two or more classes can be further combined by color coding when displayed, independent of their level. Keeping in mind that L-band radar will be sensitive to vegetation biomass, spacing of woody elements, degree of flooding under the canopy and terrain relief, we have constructed a vegetation map with twenty themes in six color groups. Within each group the map layers are stacked so that classes of lower biomass are on top of classes with greater biomass. The vegetation groups are described below:

5.1 Terra Firme Forests:

These forests which are never flooded are mapped here as three vegetation types on landscapes lower than 600 m altitude ("lowland" and "submontane" in the Veloso classification). All are geographically extensive.

Dense forests grow on well drained clay or loam in areas where there is no shortage or excess of water. They receive more than 2,200 mm of rain annually and are very high in diversity, with 150 to 300 tree species in a single hectare, which will contain 500 to 800 individual trees. Generally, no single dominant species is present. The canopy is of irregular height, generally varying from 25 to 45 m, due to the different recovery stages of small treefall gaps and the presence of occasional emergent trees. Canopy cover is continuous and the forest floor is not visible in the overflight. Many small palms and pole-size trees are found on the forest floor, the latter often depends on the occurrence of a treefall gap in order to grow into the canopy. The variability in forest structure and species diversity implies that there is no structural feature that can be used in interpreting the high resolution SAR data. Biomass exceeds the saturation point of L-band SAR (less than 100 tons/ha).

11

Open forests are also known as transition forest, this very extensive physiognomy, over one million km^2 in the Brazilian Amazon according to IBGE (1997), usually occurs where rainfall is less than 2,200 mm/yr, though some open forest with palms is also found in high rainfall areas of the western Amazon. Ecotonal open forests form an east-west oriented band in the southern Amazon Basin, sandwiched between dense forest to the north and semideciduous dry forest to the south. The number of trees per hectare is usually less than 500 and biomass is expected to be lower than in the dense forest, though occasional large emergents can keep the biomass high (Brown et al., 1995). Large emergent trees are widely spaced, sometimes giving the appearance of a two-story canopy. Shorter canopy trees are also more widely spaced than in dense forest and large light gaps are more common. The gaps are almost always occupied by lianas, bamboos or palms, or a mixture of these. The understory is clear except in the frequent gaps, which are impenetrable. Liana forests very much resemble broken up dense forests after disturbance by logging with heavy machinery, as the weight of the lianas topples many trees and favors the growth of shorter pioneer tree species in the large gaps that result. Extensive bamboo-dominated forests are restricted to 180,000 km^2 of the southwest Amazon in Brazil and Peru and are dominated by two species of spiny Guadua(Nelson & Irmo, 1998). These form mono-dominant stands in frequent gaps of 30-200 m diameter and also climb up the trees like vines. Periodic synchronous mortality of the bamboos every 30 years leads to temporary substitution by pioneer tree species, vines and a thinner bamboo (*taquari*) in the gaps. Over half of the open forests (665,000 km^2 according to IBGE, 1997) have a high density of large palms, which suggests a past history of fire penetration, particularly when babaçu palm (*Attalea speciosa*) is the dominant species. In the western to central Amazon, on poorly drained interfluvial pozdols, one finds an open forest dominated by the patau palm (*Orbignya bataua*). These are the open forests of high rainfall areas, but even patau forests are reported to catch fire (Nelson & Irmo, 1998).

The dry forests are seasonally deciduous or semideciduous. They cover 338,000 km2 of the Brazilian Amazon (IBGE, 1997), most of which is in the state of Mato Grosso, occupying a transition belt between open forest to the north and savanna to the south. Dry forest also covers the Cachimbo plateau in southern Para and forms a fire-prone transition to savannas in the state of Roraima. In Mato Grosso the dry forest is locally called cerrado, and has a clear grassy understory, though the canopy is closed as viewed from above. Biomass, tree heights and species diversity of woody elements are all lower than in the open forests. On shallow rocky soils dry forest can be completely deciduous, while on deeper clay soils they are semideciduous in the long dry season. With increasing dryness this vegetation grades into dense woodland savanna or cerradao (150,000 km^2), the

difference being that the latter has a grassy understory and even lower biomass. This vegetation is refered to as seasonal forest in figure 3.

Montane Vegetation is included as a catch-all class for all vegetation located above 600 meters (montane and high montane classes of Veloso et al, 1991). Montane forests are distinguished by their altitude and rocky soil. Mountainous regions occur within the basin to the north and at the contact with the Andes to the west. In the Brazilian Amazon, which does not abut the Andes, montane forests cover 29,000 km^2 most of which in western and northern Roraima on drainage divides with the Orinoco Basin. These forests are low in biomass. On the border between Roraima and Venezuela they are susceptible to fire penetration. Montane forest on sandstone table mountains are called "refugios" in the Veloso/RADAM classification. Montane forests on granite hills under 500 m altitude are scattered about the Guiana and Brazilian shields where many are seasonally dry with open canopies, also susceptible to fires set by lightning or escaping upslope from burning of deforested areas. Along the Andean slope the humidity increases, favoring cloud forests with mosses and epiphytes that cover the underlying rocks on the forest floor, branches and tree trunks. A better map of relief classes can be developed based on data from the soil section of the IBGE GIS. The forest category used in this study has four subcategory of dense forest, open forest, seasonal forest, and montane forest.

5.3 Savannas

In the Amazon basin, there are several open savanna areas with a variety of vegetation types. Accurate estimates of the area of savanna versus forest is not known. However, classification based on remote sensing data can readily improve these estimates. Using the IBGE classification, savanna and steppe-savanna are grouped. Each of the four biomass levels in Table 1 are shown separately and a fifth class of even higher biomass has been added, which is the area of interdigitized contact between savanna and seasonally deciduous forest or between savanna and rainforest.

Savanna types in the Amazon basin are often categorized based on their vegetation and soil characteristics. In this study, the *a priori* knowledge of the JERS-1 sensitivity to the low vegetation is the main reason for regrouping the savanna types into various levels of woody biomass. The non-forested areas of the basin are primarily located in the northeastern part of Marajo island, the Atlantic coast of Amapa, in Roraima region, south of Venezuela, and northeast of Bolivia. Overall, almost 3-4% of the Brazilian Amazon basin is covered with terra firme savanna. In general, there are two types of savanna, those of white sand which is often called caatinga and campina, and those on areas of terra firme and varzea which are on non sandy soils. The first category is also considered a

13

transitional vegetation type from forest to non-forest. In our classification, The grassland savanna is primarily open grassland without woody vegetation with basal area of 0-2 m^2 per hectare. The parkland savanna formations are encountered over the entire Brazilian Amazon. They are primarily covered with grass and shrubs with scattered trees. Some of the main parkland savannas can be found in the Marajo island, Pantanal, and the Bananal island. In parkland savanna type, one can often find numerous swampy places with scattered buriti palm (*Mauritia flexuosa*). In lower Amazon and the west part in Peru there are areas of canarana (tall grass or false cane) floating over water that can create different signature in JERS-1 imagery. This class is discussed under floodplain or inundated category in the following section. The open woodland savanna can be found in Amapa, Roriama, Para, and Maranhao. These are vegetation formations with higher density of trees and palms. The last type is forested savanna or Cerradao. This is a transitional vegetation type with a lower number of species and with closed canopy. The biomass is higher than the open forest savanna and is comprised of deciduous and semi-deciduous species.

5.4 Inundated Vegetation

This class includes the seasonally flooded vegetation of river floodplains. Muddy and black water river floodplains (varzea and igapu) are not segregated; rather there are five classes based on biomass: (1) herbaceous annuals and grasslands, (2) shrublands, (3) buriti palm (*Mauritia flexuosa*) swamps, (4) open canopy, and (5) closed-canopy alluvial forests. The first three vegetation types are considered primary successional in the Veloso et al. (1991) classification. The buriti palm swamps mapped by IBGE are an open vegetation limited to the upper Guapore River at the juncture of Rondonia, Mato Grosso and Bolivia. Field checking in extensive overflights has shown that buriti palm swamps are in fact much more common, but are classified with white sand forests or alluvial forests. Alluvial forests are classified by Prance (1979) based on chemistry of the waters and the permanence of waterlogging. The acidic black and the clear water seasonally flooded forests are known as igapu, while seasonally flooded forests of muddy neutral-pH waters are called varzea. Biomass of both vegetation types varies as a function of length of flood season, i.e. position on the inundated slope. In the middle Amazon region varzea forests grade into grassland as one moves downslope, but this is not the case in the upper Amazon, where the lowest varzea vegetation is an open viny forest called chavascal or occasionally a low shrubland with smooth canopy. Igapu forests never grade into grassland downslope, but trees become more widely spaced and shorter. Igapu forests are susceptible to burning in the low water season if their soils are sandy. Small burned

14

patches with standing dead trees over water may be distinguishable with radar. This is certainly the case for standing dead trees in two shallow hydro reservoirs: Balbina 150 km north of Manaus and Samuel, just east of Porto Velho.

Various types of large grasses which are generally called canarana can be found near the varzea forests over and around lakes. These areas often show up very bright in JERS-1 images during the wet season and can be easily confused with inundated forests. These types of savanna often occur in the lower part of the Amazon between the mouth of Xingu river and the Amazon river. They can also be found in some regions of Peru, Bolivia, and Columbia with slightly different species. In some regions of inundated savanna, because of the fertile soil and annual renewed sediments, these areas have potential for cultivation and plantations.

Primary successional formations on landscapes under fluvio-marine influence are also considered inundated vegetation types here. Two classes are shown in the RADAM map in figure 3: (1)herbaceous communities (salt marshes and dune vegetation) and (2) tidal flood forests, including mangrove swamps. Due to differences in biomass, structure and canopy smoothness, radar may separate mangrove forest from other coastal forests, but these are not available as separate vegetation types in the GIS.

Mangroves occur in estuarine region of Amazonia in areas which are flooded daily by brackish water. The formation of mangrove is well known. The vegetation structure type is very uniform, and often dense. The areas near the mouth of the river and in the coast of Marajo island extending to coast of Guiana are full of red mangrove (Rhizophora mangle), the most typical species of the Brazilian mangrove. The homogeneity of vegetation and almost all year long water underlying trees makes them to appear with different textural features than the terra firme forests and other inundated forest types. The areas that are covered by mangrove along the coast are small and may not ever show up in the 1 km JERS-1 data. Based on the a priori knowledge of JERS-1 data, we have chosen 7 class types of inundated vegetation: 1) herbaceous (including coastal communities), 2) shrubland, 3) open forest, 4) closed forest, 5) palm swamp, 6) canarana, and 7) mangrove.

5.5 White sand vegetation

Four biomass classes are mapped, as listed in table 1 and shown in figure 3. The two more open formations(campina and campina shrubland) are very extensive in interfluvial areas inland from the shores of the middle Rio Negro and the lower Rio Branco. Outliers are found in the southwest Amazon just north of the town of Cruzeiro do

15

Sul, where they show clearly in the 100m resolution L-band SAR. Tall closed canopy forest on white sand (caatinga or campinarana) is also associated with poorly drained interfluvial areas with tabular or weakly incised relief, common in the northwest Amazon. Number of trees per hectare ((10 cm DBH) can exceed 1000 individuals and canopy height is 15-25 meters. Most tree crowns are small, leading to a fine-grain texture in stereo air photos. In optical images campinarana forest shows a slightly lower NDVI and higher shade content of the pixel, than dense forest. Campinarana grades into an open woody formation interspersed with bare sand, a vegetation resembling that found on coastal dunes. The fourth class is the interdigitized contact zone of any white sand formation with terra firme forest on clay soil.

5.6 Anthropogenic vegetation

Anthropogenic vegetation refers to vegetation formations resulted from forest conversion by human disturbance. According to Veloso (1991) and IBGE classification there are four types: secondary successional stages, agriculture, pasture and tree plantation. In this study, we will focus on the secondary forests because of their importance and abundance in the basin and low vegetated nonforest lands such as pasture and some crops. Other vegetation types such as crops, and plantations are either not recognized in 1km JERS-1 classification or mixed with one of the above classes.

The areas mapped by IBGE as secondary vegetation cover 98,000 km2, mostly located in two very old agricultural frontiers: the Bragantina Zone east of Belem and the open babacu palm stands of Maranhao. The map does not show all secondary forests. Fearnside (1996) estimated that secondary forests covered 47.6% of the deforested part of the Amazon in 1990 but had an average age of less than 10 years. As of 1994 the deforested Brazilian Amazon exceeded 500,000 km2, according to an unpublished study undertaken by the National Space Research Institute (INPE) and released to the press in 1997. Twelve-year-old secondary forests 90 km north of Manaus, with above ground biomass exceeding 100 tons, are clearly distinguishable by their lower backscatter in the JERS-1 100 m data.

6. Results and Discussion

Before classifying the image, the separability of land cover classes for each category of forest, savanna, inundated vegetation, and white sand vegetation using all combination of textures is computed. The anthropogenic classes of secondary forests and nonforest are mixed with forest and savanna categories respectively. During this process,

the number of textures and separable classes are optimized for final classification . The separability is computed using the B-distance as the number and combination of texture measures change. The separability is measured relatively between 0 and 2 with 0 corresponding to no separability and 2 to maximum separability.

To make the selection of training areas as accurate as possible, we registered the RADAM map with the JERS-1 mosaic and extracted the backscatter and texture measures for each class as indicated on the map. During the selection of training areas, we avoided those cases where the RADAM class types did not match with the general characteristics of the radar image suggesting the possible misclassification of RADAM map. Furthermore, the water class was not included in our analysis. Nevertheless, this class was separated from savanna and pasture land covers by thresholding the backscatter and the variance.

6.1.a Forest

Table 2.a shows the backscatter amplitude and texture characteristics for forest class types averaged over 10 training sites. We have included secondary forests among forest types because of the high probability of being confused as forests in JERS-1 data. Among forest classes, the amplitude in byte (between 0 to 256 gray values) and/or backscattering coefficient in dB alone are not sufficient to separate the forest types. The mean backscatter may separate dense forest from some secondary or open forests, however the total separability does not exceed 0.8. This confirms previous results obtained from the analysis of SIR-C (Shuttle Imaging Radar C) over tropical forests(Saatchi et al., 1997; Rignot et al., 1997). As the density of forest changes from dense to secondary and open forests, the variance and texture diverge, and thus contributing to the discrimination. Montane forests have higher variance, contrast, and entropy than other classes. Seasonal forests (deciduous and semi-deciduous), not having any specific structural information in SAR data have less discriminating texture information and therefore, higher probability of being confused as other forest classes such as dense, open, or secondary forest.

By adding various textures, the separability increases till it maximizes by using all measurements. Table 2b. shows the B-distance computed using data from training sites. The results provide an indication of the performance of all textures in separating forest classes (average separability of 1.954). A dimensional analysis of all measures, not shown here because of space consideration, indicates that mean, texture (coefficient of variation), and variance are the most important predictor variables for discriminating forest classes.

6.1.b Inundated Vegetation

Inundated vegetation types have a very distinct characteristic in JERS-1 images. This is primarily due to the high backscatter as a result of penetration in the forest canopy and double bounce reflection from the underlying water or moist surface. However, as inundated vegetation vary in type, structural characteristics, and the seasonality of the water level, the radar backscatter alone is not able to discriminate class types. Furthermore, the JERS-1 images are acquired during the low water of the Amazon river when most seasonally inundated vegetation along the Amazon river and its tributaries have low water. In this condition, only those forest types that differ in structure from their surrounding forests can be discriminated in texture measurements. Table 3a shows the backscatter and texture characteristics of seven different classes in this category. The low mean backscatter of herbaceous and shrubland types are because of either low water condition or low vegetation and thus small double bounce or volume scattering respectively. The B-distance computed for mean backscatter is about 1.5, indicating the high performance of backscatter in discriminating inundated vegetation.

Table 3b shows the B-distance computed when all texture features are used. The average separability is 1.847 implying the increasing contribution of textures in discriminating classes in this category. The results indicate that most classes are easily separated and the confusion is only significant when discriminating herbaceous from shrublands and open from closed and palm types. Note that the canarana class type in Peru is not in the RADAM map of Brazilian Amazon and has been extracted from our knowledge of the area.

6.1.c Savanna

The characteristics of savanna class types and deforested pasture or crops are shown in table 4a. Since savanna class types are selected in increasing amount of woody biomass, the mean backscatter appears to be the best channel to separate them. The average B-distance computed for the mean backscatter is 1.7, implying a high performance in discriminating the classes. The separability between deforested and water with the grassland savanna is 1.2 and 1.4 respectively. The limited dynamic range of JERS-1 data (18 dB) and the insensitivity of L-band data to short vegetation and small roughness cause these classes have low backscatter. By adding the texture measures in the computation, the separability improves and approaches the average value of 1.898. Texture measures carry information about the inhomogeneity of grassland savanna, the homogeneous smooth water surface, and the geometric and edge effects of deforested land use that may not appear in backscatter data. However, including texture measures indicate that the grassland savanna still has a high probability of being confused with deforested landscapes. The

mixed savanna and dense woody savanna have similar structural characteristics and are not easily discriminated.

6.1.d White Sand Vegetation

Most white sand vegetation have similar backscatter characteristics as the savanna vegetation. The four classes are also based on biomass formation and tree densities. According to table 5a, the mean backscatter is the strongest discriminating measure for grassland, open and closed campinaranas. The mixed campinarana appears more homogenous in JERS-1 texture measures with lower variance and contrast but similar backscatter as closed campinarana. The B-distance in table 5b shows that by using all texture measures, the possibility of separating all classes of white sand vegetation is high (average B-distance of 1.83).

The B-distance test for class separability for each individual category demonstrated the performance of texture measures in discriminating various class types. The dimensional analysis by adding texture measures and changing the combinations shows that a maximum separability is achieved by only a subset of texture measures. Figure 4 demonstrates this for four categories of land cover types and when all classes are used in the calculation of B-distance. The first measure in each category is the mean backscatter, however, the additional combination of measures may differ for each category. By using, the average B-distance for the mean backscatter (approximately 1.5) in equation (11), the probability of correct classification for each category is larger than 80%. When all classes are used together, the probability drops to 43% (average B-distance of 0.40). This result indicates, that even though the JERS-1 mean backscatter may provide acceptable classification for each category but the performance is poor when discriminating all classes. In particular, our analysis showed that the white sand vegetation types were all confused with forest or savanna types. Table 6 shows the B-distance computed when all classes are combined. The most obvious results are: 1) confusion of herbaceous and shrubland inundated vegetation with grassland savanna, 2) confusion the closed woody savanna with open forest, 3) lack of separability between palm swamps and terra firme forest types or closed and open inundated vegetation, 4) confusion of seasonal forest with other forest types, 5) confusion of parkland savanna with other class types, and 6) high confusion of white sand vegetation types with savanna and forest class types.

As a result of this analysis, we removed the white sand category, and seasonal forest, and combined parkland and herbaceous savanna, and palm swamp with open inundated forest, shrubland and herbaceous inundated vegetation from the classification procedure. Table 7 shows the B-distance among 14 land cover types including the water

class. The average B-distance increased to 1.58 corresponding to approximately 85% accuracy in classification.

6.2 Classification Accuracy

One of the main issues in large scale land cover classification is assessing the accuracy of the results against limited and often unreliable information on global land cover. In this study, we have chosen three methods to validate the thematic information extracted from the classification of 1 km resolution JERS-1 data. These methods are: 1) the accuracy of classification algorithm as applied to the training and test sites, 2) large scale comparison of the classification against the RADAM derived map as a potential ground truth, and 3) comparison with the 1 km AVHRR global land cover classification recently produced at the University of Maryland and reported in this issue (Hansen et al., 1998).

The two stage classifier described in section 4.3 has been used to classify the 1 km JERS-1 mosaic image for the vegetation types of the Amazon basin. Using a sample set of training areas for forest, savanna, inundated vegetation, nonforest (deforested areas), and water, first a classification map was generated from the 1 km mean backscatter data. The MAP classifier was able to separate the 5 class types with approximately 75% accuracy when used on the training and test data sets. The results from section 6.1 indicate that once these general classes are identified, the radar backscatter and texture measures can further segment these classes into their subcategories.

The second stage of classification involved a hierarchical decision rule method by thresholding the mean texture measures from the tables given in section 6.1. The decision rule was applied to 14 classes. All decision rules start with the *a priori* vegetation map derived from the mean backscatter in the first stage and subdivides the categories to sub categories. The flowchart in figure 5 shows the decision rule flow for further classifying the 5 classes to 14 subcategorizes. In this figure, we have shown only the name of the texture measures used for identifying each class type. The numerical values used in the decision rule are extracted from tables 2a-5a by considering the mean and standard deviation of each quantity over the training sites.

The classification map of the 1 km image mosaic is given in figure 6. The accuracy of classification is given in terms of confusion matrix in Table 8. The accuracy is calculated by the number of training sites correctly classified. Since the training sites are obtained from the 100 meter JERS-1 data, each represent one pixel in the 1 km data map. Even though, this does not represent the overall accuracy of the map, however, it shows the performance of the classification methodology. The accuracy according to the confusion matrix in table 8 is 78%. Majority of misclassified sites are those that had lower

20

separability with other classes in the B-distance matrix shown in table 7. Among the open forest sites that are taken from liana and bamboo forests in the southwest of the basin 7 are classified correctly and the rest are identified as dense forest, secondary forest, and closed canopy woody savanna. Montane forests are identified correctly (90% accuracy), indicating that texture measures are capable of separating cover types that are often misclassified in backscatter data due to the topography effects. The errors in woody savanna classes are higher than the forest types because of often the loose definition of woody savanna classes in RADAM map (biomass density of woody savanna is not explicitly quantified).

6.3 Comparison with RADAM derived vegetation map

The comparison with the RADAM map is performed visually for assessing the general patterns of land cover types. Because of the scale difference between two maps, the pixel to pixel comparison as a result of map registeration introduces resampling error. Overall, two maps show similar patterns of land cover types.

The general patterns of open forests in the Eastern part of the basin are identified. However, they are confused with dense, the montane forests. In the south western part of the basin in the state of Acre, Brazil, Peru and Bolivia, the liana and bamboo forests mixed with evergreen forests are identified correctly as the open forest. These areas of open forest generally agree with areas of liana and bamboo forests as shown in Nelson (1994) results. In the Northeastern Brazil, most classes are identified as montane forests, mixed with some open forests in French Guiana, Surinam, and Guyana. Since the RADAM map does not identify any open forests in the region, we are not certain about the accuracy of the classification in this area. The montane forests in JERS-1 result does not follow the characteristics of montane forests in RADAM map. In JERS-1 map areas with lower than 600 m altitude are also identified as montane forests because of the effect of topography on variance and contrast texture measures.

According to the confusion matrix in table 8, anthropogenic classes such as deforested areas and the secondary forests are identified with 70% accuracy. Comaprison with RADAM map shows that the confusion is between grazing pasture in Rondonia and Para states in Brazil with grassland savanna and open forests respectively. At 1 km scale, most deforested areas and secondary forests appear in subpixel scale and thus easily misclassified. However, the general location and patterns of these classes match with the RADAM land cover map and our general knowledge of the occurance of these classes in regions under intense land use change and deforestation.

In the savanna category, all subcategory training sites are identified with high accuracy. However, in comparison with the RADAM map, the patterns do not always coincide. According to Veloso (1991) the savanna subcategories are defined based on the amount of the woody vegetation. Since the density of trees in each pixel can impact the SAR backscatter and texture, the misclassification of general patterns may have been caused by the loose definition of subcategories. Moreover, the RADAM map was generated from the visual interpretation of RADAMBRASIl airborne radar survey, operating at X-band. At X-band the radar return saturates at lower woody biomass than JERS-1 L-band radar, and thus maps the landscape patterns differently. This is particularly true when separating the parkland savanna from grasslands and open woodlands.

The classification shows a high performance over inundated land cover types. Even though, the JERS-1 images were acquired during the low water season, the texture measures were able to identify most inundated or floodplain vegetation along the Amazon river and its tributaries. The confusion is mainly in separating the coastal herbaceous vegetation from inland herbaceous and shrubs. The open and closed inundated vegetation also show some degree of misclassification primarily due to the radar response to the underlying water level. The subcategories of the inundated vegetation are often most difficult to identify because of their temporal characteristic of class types. For example, the areas along the Eastern coast, and the Maraju island show slightly different patterns as compared to the RADAM map. The areas of herbaceous swamps are mixed with grassland savanna. The marshland and low vegetated swamps are better discriminated when higher frequency radar channels are added. For example, C-band data acquired during the SIR-C (Shuttle Imaging Radar C) showed high sensitivity to herbaceous inundated vegetation (Hess et al., 1995). Note that one of the main sources of error between two maps is in areas along the edges of land cover types and their general landscape patterns. This is often true when comparing large scale maps derived from two different sources such as remote sensing instruments or aireal photopgraphy because each instrument's signal responds differently to the surface or vegetation characteristics.

6.3 Comparison with AVHRR Based 1km Map

A comparison of our map with the latest AVHRR based 1 km vegetation map would thoroughly verify the classification and reveal information which can be used for future synergism and fusion of optical and microwave remote sensing data and techniques. For comparison, we have used the land cover classification based on 1km AVHRR data for 1992-93 reported in the current issue (Hansen et al., 1998). This AVHRR classification is based on a "continuous fields" approach of vegetation properties which includes gradients

22

and hetrogeneities of vegetated land surface. A linear mixture model is applied on monthly averaged NDVI data in order to estimate proportional cover for three important vegetation characteristics: life form (present woody vegetation, herbaceous vegetation, and bare ground), leaf type (percent needleleaf and broadleaf), and leaf duration (percent evergreen and deciduous). The classified vegetation map has all 17 classes of IGBP (International Geosphere Biosphere Project) legend. Figure 7 shows the AVHRR 1 km land cover map of the Amazon basin with fifteen classes as a result of merging two low vegetation classes in the global map. The classification is designed for global land cover types and therefore it does not include or necessarily corresponds with the usual land cover types used in the JERS-1 or RADAM map of the Amazon basin. However, by merging cover types and interpreting the difference in terminology used in each map, one can compare two images for general land cover types.

To start with, we resampled and co-registered the JERS-1 map with the AVHRR map. By comparing only forest, savanna herbaceous, woody savanna, deforested, floodplain vegetation, and open water, we were able perform a comparison on a pixel to pixel basis. The merged classes between the two maps are shown in table 9. The area covered by each class in either AVHRR or JERS-1 maps and the difference between the surface areas covered by each class in the maps are shown in table 10. In order to exclude the areas of Andes and to focus on the areas with the least topographical effects, we extracted an area of 2000 km by 2000 km in the middle of maps. Overall, the agreement between two forest cover types was close to 95% of the entire forested areas. The herbaceous savanna has larger surface area in AVHRR image than in JERS-1. Visually most savanna areas are classified similarly in both images. The main difference is due to the herbaceous floodplains class along the main channels of the Amazon in the JERS-1 map and the savanna in AVHRR map. This difference is also seen when comparing the floodplain vegetation. The inundated areas are better distinguished in JERS-1 data and thus covering more surface area. AVHRR map has the permanent wetland class that often refers to areas of open conopy. Comparison with the RADAM map in figure 3 indicates that the AVHRR map does not separate the closed canopy woody savanna from the evergreen broadleaf forest accurately. This may partially be due to the fact the classification was designed for a global land cover map and not for the Amazon basin specifically. Comparing the areas of open forests and secondary vegetation in AVHRR map with the RADAM map also indicates that these cover types are classified as evergreen forests. In particular, in the province of Para in northeast of Brazil where a large portion of the forest is either intensely degraded or as secondary forests, the AVHRR map is not correct. Other vegetation maps based on the AVHRR data that are designed for the South American

23

vegetation types show better distinction among classes and more suitable for comparison with the JERS-1 data (Stone et al., 1994).

Note that one of the main distinction between the two maps is the better delineation of land cover types in JERS-1 map. For example, the deforested areas have 13% difference which are mainly due to the finer distinction of the edges and boundaries of this class in JERS-1 map. This is primarily due to the fact that the 1 km JERS-1 mosaic map was generated from aggregating a finer resolution image data (100 m). The same result can be achieved if a finer resolution optical data such as Landsat were used in generating the 1 km map (DeFries and Thownshend, 1994).

7. Concluding Remarks

In this paper, we have demonstrated that single channel high resolution radar data can successfully be used for regional scale mapping of land cover types. The data were acquired in a short period over the Amazon basin where cloud cover and changes of land cover and/or land use can hinder the use of other high resolution data sets such as Landsat imagery. Our main objective was to develop a methodology that can produce thematic information from radar remote sensing in a repeatable fashion. The use of texture measures augments the single channel radar data by adding the statistical information about the signal that can be readily used in any standard classification algorithm. In this study, we have shown that a two stage classifier based on a maximum likelihood technique and decision rule can provide detailed information about the land cover types. As input parameters to the classifier such as more radar channels (e.g. other frequencies, polarizations, and higher order texture features) increases, the classification accuracy and number of land cover types can increase.

The acquisition, processing, calibration, mosaicking, resampling, and classification of more than 1500 JERS-1 images have produced a 1 km map of the Amazon basin with 14 land cover types. The accuracy of classification is approximately 78%. Starting with 20 class types from a more detailed map of RADAM, we have shown that the JERS-1 data from the dry season can separate Amazonian cover types based on their structure, biomass, and moisture condition. The class types were chosen according to the needs of mapping dominant vegetation types and the sensitivity and dynamic range of the JERS-1 data. In the case of inundated vegetation, the same image mosaic from the wet season will improve the classification accuracy.

The classification methodology in this paper was aimed to demonstrate both the capability and insensitivity of the JERS-1 data and the texture measures to map a desired set of land cover types in the Amazon basin. For example, the white sand herbaceous and woody vegetation can not be directly mapped by radar images. This result suggests that the synergism of radar data and other remote sensing insturments that are sensitive to soil type.

Acknowledgment

References

Anys, H., and He, D-C. 1995. evaluation of textural and multipolarization radar features for crop classification, *IEEE Geosci. Remote Sens.*, 33:1170-1181.

Brazil. 1972-1982. Projeto RADAMBRASIL. Levantamento de Recursos Naturais Volumes 1-27.

Brown, I.F.; Martinelli, L.A.; Thomas, W.W.; Moreira, M.Z.; Ferreira, C.™c. & Victoria, R.A. 1995. Uncertainty in the biomass of Amazonian forests: an example from Rondonia, Brazil. Forest Ecology and Management 75: 175-189.

Brown,S. and Lugo, A.E. 1984, Biomass of tropical forest: a new estimate based on forest volume, *Science* 223: 1290-1293.

DeFries, R., Townshend J., and Hansen, M. 1997, submitted, Continuous fields of vegetation characteristics at the global scale, *Journal of Geophysical Research*.

DeFries R., and Thownshend, J. 1994.
Fearnside, P.M. 1996. Amazonian deforestation and global warming: carbon stocks in vegetation replacing Brazil's Amazon forest. Forest Ecology and Management 80: 21-34.

Foody, G.M., and Curran, P.J. (1994), Estimation of tropical forest extend and regenerative stage using remotely sensed data, *J. of Biogeorahy*. 21:223-244.

Hansen, M., DeFries, R. and Townshend, J., (1998) submitted , 1 km global land cover classification using a supervised decision tree classifier, special issue of *Int. J. Remote Sens.*

Hess, L.L., Melack, J.M., Filoso, S., and Wang, Y. 1995. Mapping wetland hydrology with synthetic aperture radar, *IEEE Trans. geosci. Remote Sens.* 33, 896-904.

Houghton, R.A. 1991. Tropical deforestation and atmospheric carbon dioxide. *Climate Change* 19:99-118.

Houghton, R.A. 1995. Land-use change and the carbon cycle, *Global Change Biology*, 1:275-287.

IBGE (Instituto Brasileiro de Geografia e Estatìstica). 1997. Diagnûstico Ambiental da Amazonia Legal. CD-ROM produced by IBGE. Rio de Janeiro.

Instituto Nacional de Pesquisas Espaciais (INPE), 1992. Deforestation in Brazilian Amazonia, INPE, Sao Jose dos Campos, Brazil.

Justice, C.O., Thownshend, J.R.G. 1994. Data sets for global remote sensing, leasson learned, *Int. J. Remote Sens.*, 3621-3639.

Luckman, A., Baker, J., Kuplich, T.M., Yanasse, C., and Frery, A.C. 1997. A study of the relationship between radar backscatter and regenerating tropical forest biomass for spaceborne SAR instruments, *Remote Sens. Environ.*, 60:1-13.

Malingreau, J.P., Archard, F., D'Souza, G., Stiibig, H.J., D'Souza, J., Estreguil, C., and Eva, H. 1995. AVHRR for global tropical forest monitoring: The lessons of the TREES project. *Remote Sensing Reviews* 12:29-40.

Myers, N. (1988), Tropical forest and their species going, going...?, in *Biodiversity* edited by E.O.Wilson, National Academy Press, pp. 28-35.

Myers, N. (1992), *Conserving Biodiversity: A Research Agenda for Development Agencies*, Washington, D.C.; National Academy Press.

Moran, E.F., Brondizio, E., Mausel, P., and Wu. Y. (1994), Integrating Amazon vegetation, land-use, and satellite data, *Bioscience* 44: 329-338.

Nelson, B. and Irmo, B. 1998, Mapping Bamboo Forest in the Amazon Basin, submitted.

Nelson, B.

Nelson, R. and Holben, B. (1986), Identifying deforestation in Brazil using multiresolution satellite data, *Int. J. Remote Sens.* 7: 429-448.

Pires, J.M. and Prance, G.T. (1981), The vegetation types of the Brazilian Amazon, in 109-145.

Prance, G.T. (1979), Notes on the Vegetation of Amazonia III. The terminology of Amazonian forest types subject to inundation, *Brittonia*, 31(1):26-38.

Richards, P.W. (1952), *The Tropical Rain Forest*, Cambridge Univ. Press.

Rignot, E., Salas, W., and Skole, D.L. 1997. Mapping deforestation and secondary growth in Rondonia, Brazil, using imaging radar and thematic mapper data, *Remote Sens. Environ.*, 59:167-179.

Rignot, E. and Chellappa, R. 1993, Maximum *a posteriori* classification of multifrequency, multilook, synthetic aperture radar intensity data, *J. Opt. Soc. Am.* 10:573-582.

Saatchi, S.S., Soares, J.V., and Alves, D.S., Mapping deforestation and land use in Amazon rainforest using SIR-C imagery, submitted to *Remote Sens. Environ.* , February,1996a.

Saatchi, S.S., and Rignot, E. 1996. Classification of boreal forest cover types using SAR images, *Remote Sens. Environ.* 60:270-281.

Sader, S.A. (1987), Forest biomass, canopy structure and species composition relationships with multipolarization L-band synthetic aperture radar data, *Phtogramm. Eng. Remote Sens.* 53(2):193-202.

Sioli, H. (1984), *The Amazon, limnology and landscape ecology of a mighty tropical river and its basin*, Dr. Jung Publishers, Netherlands.

Siquiera et al.,

Skole, D.L., Chomentowski, W.H., Salas, W.A., and Nobre, A.D. (1994), Physical and human dimesions of deforestation in Amazonia, *Bioscience* 44: 314-322.

Skole, D.L. and Tucker, C.J. (1993), Tropical deforestation and habitat fragmentation in Amazon: Satellite data from 1978 to 1988, *Science* , 260:1905-1910.

Stone, T.A., Schlesinger, R., Houghton, R.A., and Woodwell, G.M. (1994), A map of the vegetation of South America based on satellite imagery, *Photogram. Eng. Remote Sens.* 60(5):541-551.

Swain, P.H., and King, R.C., (1973), Two effective feature selection criteria for multispectral remote sensing, in *Proc. 1st Int. Joint Conf. Pattern Recognition*, 536-540.

Townshend, J.R.G. and C.O. Justice, Selecting the spatial resolution of satellite sensors required for global monitoring of land transformations, *Int. J. Remote Sens.* , 9, 187-236, 1988.

Thownshend, J.R.G., Justice C., and Kalb, V. (1987), Characterization and classification of South America land cover types using satellite data, *Int. J. of Remote Sens.* 8(8):1189-1207.

Tucker, C.J., Holben, B.N., and Goff, T.E. (1984), Intensive forest clearing in Rondonia, Brazil as detected by satellite remote sensing, *Remote Sensing Env.* 15: 255-261.

Tucker, C.J., Thownshend, J.R.G., and Goff, T. (1985), Continental land cover classification using NOAA-7 AVHRR data, *Science*, 227:369-375.

Ulaby, F.T., Kouyate, F., and Brisco, B. 1986. Textural information is Sar images, *IEEE Trans. Geosci. Remote Sens.*, 24:235-245.

Veloso, H.P.; Rangel Filho, A.L.R.& Lima, J.C.A. 1991. Classificâo da Vegetâo Brasileira, Adaptada a um Sistema Universal. IBGE. Rio de Janeiro. 123 pp.

Figure Captions:

Figure 1. The JERS-1 low water coverage of the Amazon basin in 1995.

Figure 2. JERS-1 radar backscatter mosaic image of the Amazon basin. The mosaic is developed using 1500 JERS-1 images at 100 m resolution.

Figure 3. IBGE vegetation classification of Brazilian Amazon based on the RADAMBRASIL project (IBGE, 1997). Several vegetation types are merged in order to create a map with less classes and suitable for examining the statistical characteristics of JERS-1 data. The land covert type legend is given in table 1.

Figure 4. The separability of land cover type categories in terms of B-distance as computed by increasing the number of texture measures.

Figure 5. Flow of textuyre decision rule for the second stage of the classifier. The acronyms for texture measures and classes are given in the caption of Table 2a and 6 respectively. Four intermediate class types are introduced ini this flow: sav-w (woody savanna), sav-nw (non-woody savanna), fld-ft (floodplain forest), ft-txt (textured forest).

Figure 6. Map of land cover types of the Amazon basin obtained from JERS-1 mosaic and texture measures. The map includes 14 classes which are idensitified in the figure legend.

Figure 7. AVHRR based 1 km land ocver types of the Amazon basin, extracted from the the global land cover map.

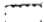Table 1. Land cover type legend for the RADAM map of figure 2.
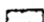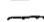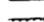
⬚	Savanna-Estape (grassland and shrubland)
⬚	Savanna-Estape (parkland)
▨	Savanna-Estape (open woodland)
▮	Savanna-Estape (closed canopy woodland)
	Mixed Savanna With Seasonal or Evergreen Forest
⬚	Coastal Vegetation (herbaceous)
▮	Coastal Vegetation (mangrove and restinga)
▢	Inundated Vegetation (herbaceous and annual grass)
▨	Inundated Vegetation (shrubland)
▮	Inundated Vegetation (palm swamps and open canopy)
▮	Inundated Vegetation (closed canopy alluvial forest)
⬚	White Sand Vegetation (grassland and shrubland)
⬚	White Sand Vegetation (open forest)
▨	White Sand Vegetation (dense forest)
▮	White Sand Forest Mixed With Evergreen Forest
▮	Montane and Upper Montane Forest
▮	Secondary Forest
▮	Seasonal Forest (lowland and submontane)
▮	Open Forest (lowland and submontane)
▮	Dense Forest (lowland and submontane)

Table 1. Land cover type legend for Figure 3.

Table 2a. JERS-1 texture characteristics of training sites for land cover type classes in forest catagory.
The acronyms for texture measures are: MS (mean), VAR (variance), TEX (texture or coefficient of variation), ENT (entropy), ENE (energy), CON(contrast), SKW (skewness), and KUR (kurtosis).

class	MS	VAR	TEX	ENT	ENE	CON	SKW	KUR
dense	123	17.2	0.0051	1.18	0.078	518	0.091	1.37
open	110	69.4	0.0257	1.42	0.044	1789	0.137	2.68
seasonal	118	30.9	0.0097	1.28	0.061	879	0.178	2.14
montane	107	664.1	0.265	1.71	0.022	12432	0.545	2.72
secondary	110	47.7	0.0174	1.35	0.052	1269	-0.024	2.91

Table 2b. Class separability (B-distance) of training data set using all texture measures for classes in forest catagory.
Average separability for all measurements is 1.954.

class	dense	open	seasonal	montane	secondary
dense	0.0	1.99	1.69	1.99	1.99
open	1.99	0.0	1.84	1.97	1.74
seasonal	1.69	1.84	0.0	1.99	1.68
montane	1.99	1.97	1.99	0.0	1.98
secondary	1.99	1.74	1.68	1.98	0.0

Table 3a. JERS-1 texture characteristics of training areas for land cover classes of inundated vegetation

class	MS	VAR	TEX	ENT	ENE	CON	SKW	KUR
herbaceous	83	32.4	0.024	1.258	0.066	836	0.0182	1.84
shrubland	72	31.7	0.032	1.27	0.064	838	-0.0006	2.31
open canopy	128	42.7	0.011	1.32	0.058	1152	0.23	2.69
closed canopy	158	38.7	0.009	1.31	0.057	1221	0.154	2.74
canarana-Peru	212	99.2	0.009	1.47	0.04	2700	-0.464	3.39
palm swamp	138	146.9	0.031	1.52	0.036	3374	-0.138	2.73
mangrove	123	68.9	0.0198	1.40	0.055	2102	0.049	3.61

Table 3b. Class separability (B-distance) of training data set using all texture measures for classes in inundated vegetation catagory. Average separability for all measurements is 1.847.

class	herbaceous	shrubland	open	closed	canarana	palm	mangrove
herbaceous	0.0	1.54	2.0	2.0	2.0	1.98	1.99
shrubland	1.54	0.0	2.0	2.0	2.0	1.99	2.0
open	2.0	2.0	0.0	1.32	2.0	1.69	1.26
closed	2.0	2.0	1.32	0.0	2.0	1.82	1.99
canarana	2.0	2.0	2.0	2.0	0.0	1.99	2.0
palm	1.98	1.99	1.69	1.82	1.99	0.0	1.25
mangrove	1.99	2.0	1.26	1.90	2.0	1.25	0.0

Table 4a. JERS-1 texture characteristics of training areas for land cover classes of savanna vegetation

class	MS	VAR	TEX	ENT	ENE	CON	SKW	KUR
grassland	49	19.7	0.086	1.1	0.1	557	1.05	8.89
parkland	75	187.8	0.189	1.57	0.033	3622	0.575	2.68
open woodland	82	55.3	0.047	1.32	0.058	1422	0.33	2.41
closed woodland	111	25.2	0.009	1.24	0.066	629	0.138	1.76
mixed	108	28.8	0.011	1.27	0.062	758	0.098	1.91
deforested	63	50.89	0.091	1.28	0.064	1660	1.317	6.23

Table 4b. Class separability (B-distance) of training data set using all texture measures for classes in savanna catagory. Average separability for all measurements is 1.898.

class	grassland	parkland	open	closed	mixed	deforested
grassland	0.0	2.0	1.99	2.0	2.0	1.71
parkland	2.0	0.0	1.93	2.0	2.0	1.99
open	1.99	1.93	0.0	2.0	1.99	1.97
closed	2.0	2.0	2.0	0.0	0.87	2.0
mixed	2.0	2.0	1.99	0.87	0.0	2.0
deforested	1.71	1.99	1.97	2.0	2.0	0.0

Table 5a. JERS-1 texture characteristics of training areas for land cover classes of campinarana vegetation

class	MS	VAR	TEX	ENT	ENE	CON	SKW	KUR
grassland camp	58	153.8	0.39	1.45	0.044	4005	1.61	6.49
open camp	96	98.3	0.056	1.47	0.040	2316	0.237	2.65
closed camp	116	34.4	0.012	1.28	0.061	926	0.453	2.52
mixed camp	115	26.8	0.009	1.24	0.069	695	-0.0006	1.91

Table 5b. Class separability (B-distance) of training data set using all texture measures for classes in scampinarana catagory. Average separability for all measurements is 1.830.

class	grassland	open	closed	mixed
grassland	0.0	1.81	1.99	2.0
open	1.81	0.0	1.90	1.99
closed	1.99	1.90	0.0	1.26
mixed	2.0	1.99	1.26	0.0

	ft-ds	ft-op	ft-sn	ft-mn	sav-hb	sav-pk	sav-op	sav-cl	mng	fld-hb	fld-P	fld-cl	fld-op	fld-pm	sav-mx	fld-sh	cam-hb	cam-op	cam-cl	cam-mx	ft-sd	def
ft_ds	0.00	1.96	0.75	1.40	2.00	2.00	2.00	1.96	0.37	2.00	2.00	1.74	0.76	1.16	1.79	2.00	2.00	1.67	1.15	1.68	1.90	2.00
ft_op	1.96	0.00	1.43	0.57	2.00	2.00	2.00	0.03	1.57	1.98	2.00	2.00	1.97	1.53	0.27	2.00	2.00	1.16	0.78	1.33	0.02	2.00
ft_sn	0.75	1.43	0.00	0.96	2.00	2.00	2.00	1.40	0.66	2.00	2.00	1.92	1.45	1.25	1.24	2.00	2.00	1.46	0.18	0.44	1.26	2.00
ft_mn	1.40	0.57	0.96	0.00	2.00	1.94	1.79	0.67	1.10	1.58	2.00	1.88	1.59	1.20	0.15	1.96	2.00	0.40	0.66	1.09	0.46	2.00
sav_hb	2.00	2.00	2.00	2.00	0.00	1.83	1.98	2.00	2.00	1.93	2.00	2.00	2.00	2.00	2.00	1.76	0.37	1.91	2.00	2.00	2.00	1.26
sav_pk	2.00	2.00	2.00	1.94	1.83	0.00	0.68	2.00	2.00	0.53	2.00	2.00	2.00	1.97	2.00	0.05	1.41	1.20	2.00	2.00	2.00	1.31
sav_op	2.00	2.00	2.00	1.79	1.98	0.68	0.00	2.00	2.00	0.11	2.00	2.00	2.00	1.94	1.99	0.97	1.88	0.86	2.00	2.00	2.00	1.94
sav_cl	1.96	0.03	1.40	0.67	2.00	2.00	2.00	0.00	1.56	1.98	2.00	2.00	1.97	1.55	0.39	2.00	2.00	1.24	0.73	1.28	0.06	2.00
mng	0.37	1.57	0.66	1.10	2.00	2.00	2.00	1.56	0.00	2.00	2.00	1.13	0.23	0.66	1.44	2.00	2.00	1.49	0.83	1.22	1.48	2.00
fld-hb	2.00	1.98	2.00	1.58	1.93	0.53	0.11	1.98	2.00	0.00	2.00	2.00	2.00	1.90	1.88	0.75	1.73	0.56	1.99	2.00	1.97	1.74
fld-P	2.00	2.00	2.00	2.00	2.00	2.00	2.00	2.00	2.00	2.00	0.00	2.00	2.00	1.95	2.00	2.00	2.00	2.00	2.00	2.00	2.00	2.00
fld-cl	1.74	2.00	1.92	1.88	2.00	2.00	2.00	2.00	1.13	2.00	2.00	0.00	0.89	0.44	1.99	2.00	2.00	1.90	1.94	1.98	1.99	2.00
fld-op	0.76	1.97	1.45	1.59	2.00	2.00	2.00	1.97	0.23	2.00	2.00	0.89	0.00	0.74	1.90	2.00	2.00	1.75	1.61	1.86	1.95	2.00
fld-pm	1.16	1.53	1.25	1.20	2.00	1.97	1.94	1.55	0.66	1.90	1.95	0.44	0.74	0.00	1.40	1.98	2.00	1.43	1.26	1.51	1.48	2.00
sav-mx	1.79	0.27	1.24	0.15	2.00	2.00	1.99	0.39	1.44	1.88	2.00	1.99	1.90	1.40	0.00	2.00	2.00	0.74	0.75	1.20	0.19	2.00
fld-sh	2.00	2.00	2.00	1.96	1.76	0.05	0.97	2.00	2.00	0.75	2.00	2.00	2.00	1.98	2.00	0.00	1.23	1.31	2.00	2.00	2.00	1.04
cam-hb	2.00	2.00	2.00	2.00	0.37	1.41	1.88	2.00	2.00	1.73	2.00	2.00	2.00	2.00	2.00	1.23	0.00	1.78	2.00	2.00	2.00	0.46
cam-op	1.67	1.16	1.46	0.40	1.91	1.20	0.86	1.24	1.49	0.56	2.00	1.90	1.75	1.43	0.74	1.31	1.78	0.00	1.28	1.53	1.09	1.77
cam-cl	1.15	0.78	0.18	0.66	2.00	2.00	2.00	0.73	0.83	1.99	2.00	1.94	1.61	1.26	0.75	2.00	2.00	1.28	0.00	0.29	0.63	2.00
cam-mx	1.68	1.33	0.44	1.09	2.00	2.00	2.00	1.28	1.22	2.00	2.00	1.98	1.86	1.51	1.20	2.00	2.00	1.53	0.29	0.00	1.12	2.00
ft-sd	1.90	0.02	1.26	0.46	2.00	2.00	2.00	0.06	1.48	1.97	2.00	1.99	1.95	1.48	0.19	2.00	2.00	1.09	0.63	1.12	0.00	2.00
def	2.00	2.00	2.00	2.00	1.26	1.31	1.94	2.00	2.00	1.74	2.00	2.00	2.00	2.00	2.00	1.04	0.46	1.77	2.00	2.00	2.00	0.00

Table 6. Class separability measurements in terms of B-distance when all classes and all texture measures are combined. The acronyms for class types are: ft-ds (dense forest), ft-op (open forest), ft-sn (seasonal forest), ft-sd (secondary forest), ft-mn (montane forest), sav-mx (mixed savanna), sav-cl (closed savanna), sav-op (open savanna), sav-pk (parkland savanna), sav-hb (herbaceous/grassland savanna), fld-cl (closed canopy flooded), fld-op (open canopy flooded), fld-hb (flooded herbaceous), fld-P (Peruvian canarana), fld-pm (palm swamp), cam-hb (campinarana herbaceous), cam-op (open woody campinarana), cam-cl (closed canopy campinarana), cam-mx (mixed forest campinarana), mng (mangrove), def (anthropogenic deforested).

class	ft-ds	ft-op	ft-sd	ft-mn	sav-cl	sav-op	sav-hb	fld-cl	fld-op	fld-hb	fld-P	mng	def	o w
ft-ds	0.0	1.95	1.90	2.0	1.96	2.0	2.0	1.74	1.96	1.99	2.0	1.83	2.0	2.0
ft-op	1.95	0.0	1.64	1.89	0.4	1.98	2.0	1.99	1.98	1.97	2.0	1.95	2.0	2.0
ft-sd	1.90	1.64	0.0	2.0	1.86	1.99	2.0	1.99	1.94	1.97	2.0	1.93	2.0	2.0
ft-mn	2.0	1.89	2.0	0.0	1.98	1.79	1.99	1.87	2.0	1.99	2.0	1.97	1.98	2.0
sav-cl	1.96	0.4	1.86	1.98	0.0	2.0	2.0	1.99	1.96	1.98	2.0	1.98	2.0	2.0
sav-op	2.0	1.98	1.99	1.79	2.0	0.0	1.97	2.0	1.99	1.51	2.0	2.0	1.94	2.0
sav-hb	2.0	2.0	2.0	1.99	2.0	1.97	0.0	2.0	2.0	1.92	2.0	2.0	1.26	1.72
fld-cl	1.74	1.99	1.99	1.87	1.99	2.0	2.0	0.0	1.54	1.82	1.90	1.12	2.0	2.0
fld-op	1.96	1.98	1.94	2.0	1.96	1.99	2.0	1.54	0.0	1.99	2.0	1.68	2.0	2.0
fld-hb	1.99	1.97	1.97	1.99	1.98	1.51	1.92	1.82	1.99	0.0	2.0	1.99	1.73	1.71
fld-P	2.0	2.0	2.0	2.0	2.0	2.0	2.0	1.90	2.0	2.0	0.0	2.0	2.0	2.0
mng	1.83	1.95	1.93	1.97	1.98	2.0	2.0	1.12	1.68	1.99	2.0	0.0	2.0	2.0
def	2.0	2.0	2.0	1.98	2.0	1.94	1.26	2.0	2.0	1.73	2.0	2.0	0.0	1.89
ow	2.0	2.0	2.0	2.0	2.0	2.0	1.72	2.0	2.0	1.71	2.0	2.0	1.89	0.0

Table 7. Class separability measurements in terms of the B-distance(ow stands for open water class).

Class	AVHRR Map (Merged Classes)	JERS-1 Map (Merged Classes)
Forest	Evergreen Needleleaf Forest Evergreen Broadleaf Forest Deciduous Needleleaf Forest Deciduous Broadleaf Forest Mixed Forest	Dense Forest Open Forest Montane Forest Secondary Forest
Savanna	Open Shrubland Closed Shrubland Savanna Grassland	Savanna Herbaceous
Woody Savanna	Woody Savanna	Open Woody Savanna Closed Woody Savanna
Floodplain	Permanent Wetland	Herbaceous Inundated Open Inundated Closed Inundated Canarana Mangrove
Deforested	Cropland Urban Barren, Sparsely Vegetated	Deforested
Open Water	Open Water	Open Water

Table 9. Comparison of merged land cover types in AVHRR and JERS-1 classification.

Maps	Forest	Herbaceous Savanna	woody Savanna	Floodplain	Deforested	Water
AVHHR	85.5%	7.3%	3.6%	2.6%	0.7%	0.3%
JERS-1	87.8%	1.3%	3.8%	5.7%	0.8%	0.4%
Difference	4.5%	42.3%	22.4%	59.1%	12.7%	13.8%

Table 10. Proportions of land cover types in a 2000 km by 2000 km subarea of AVHRR and JERS-1 classified maps and the percentage of pixel by pixel difference.
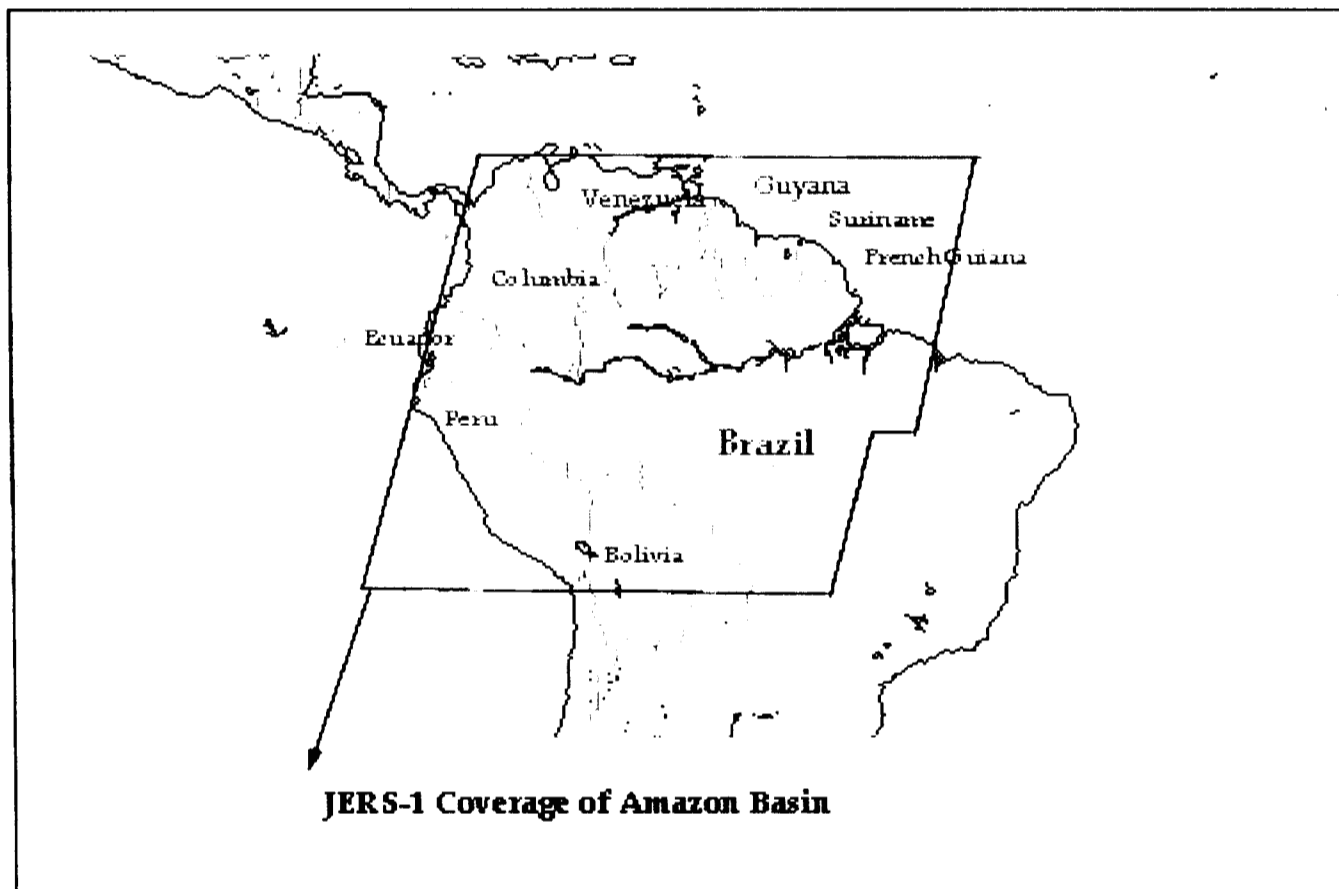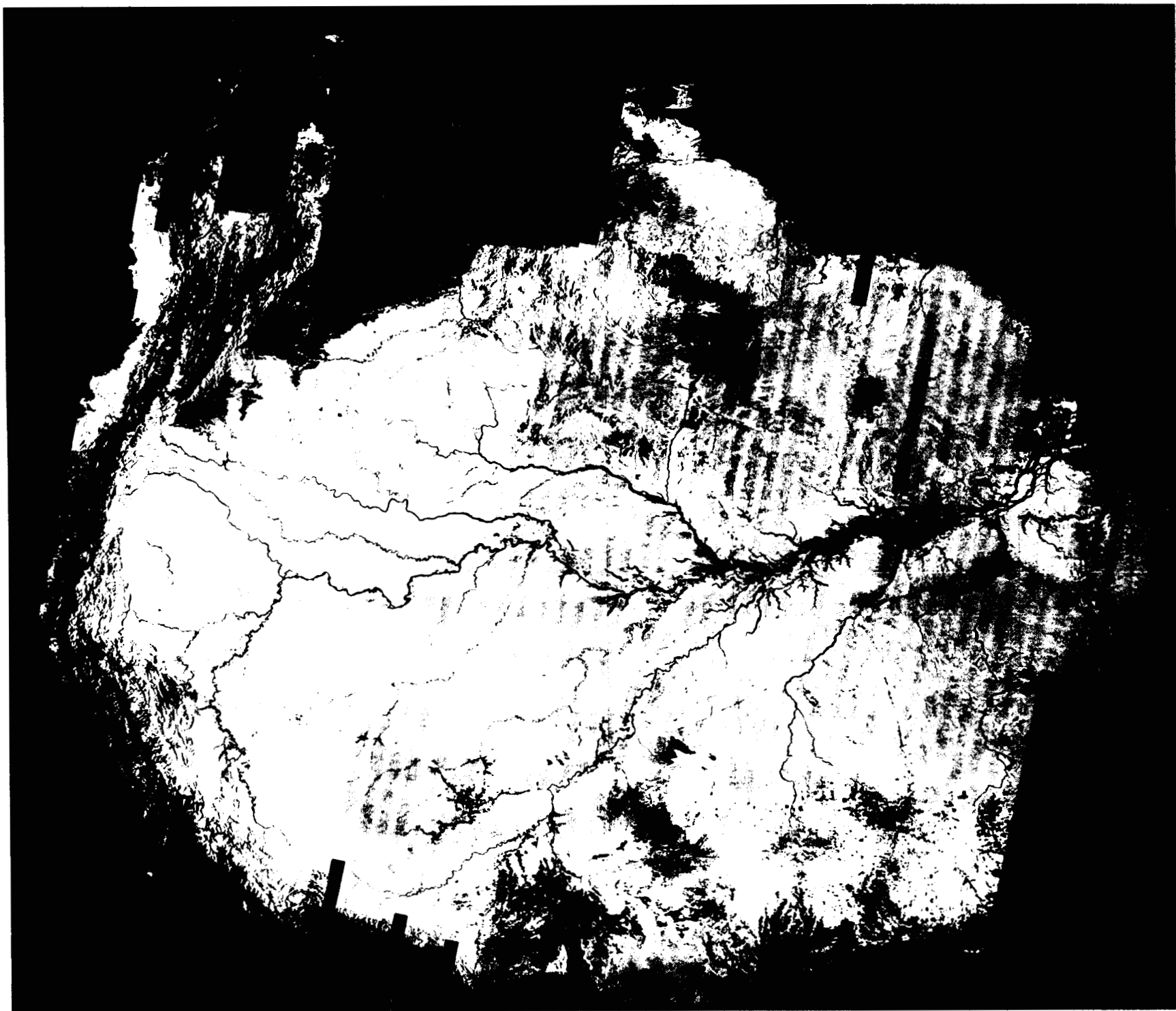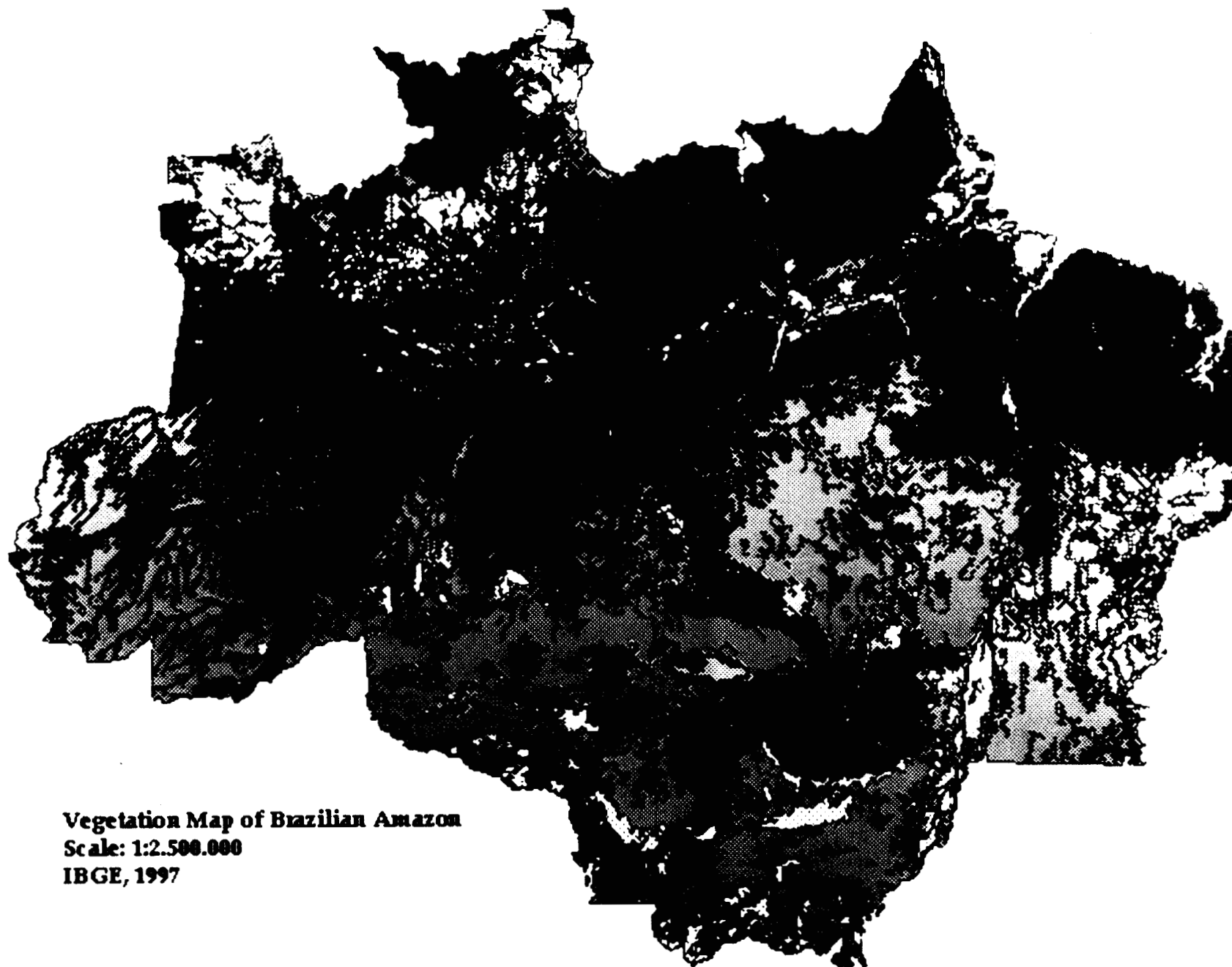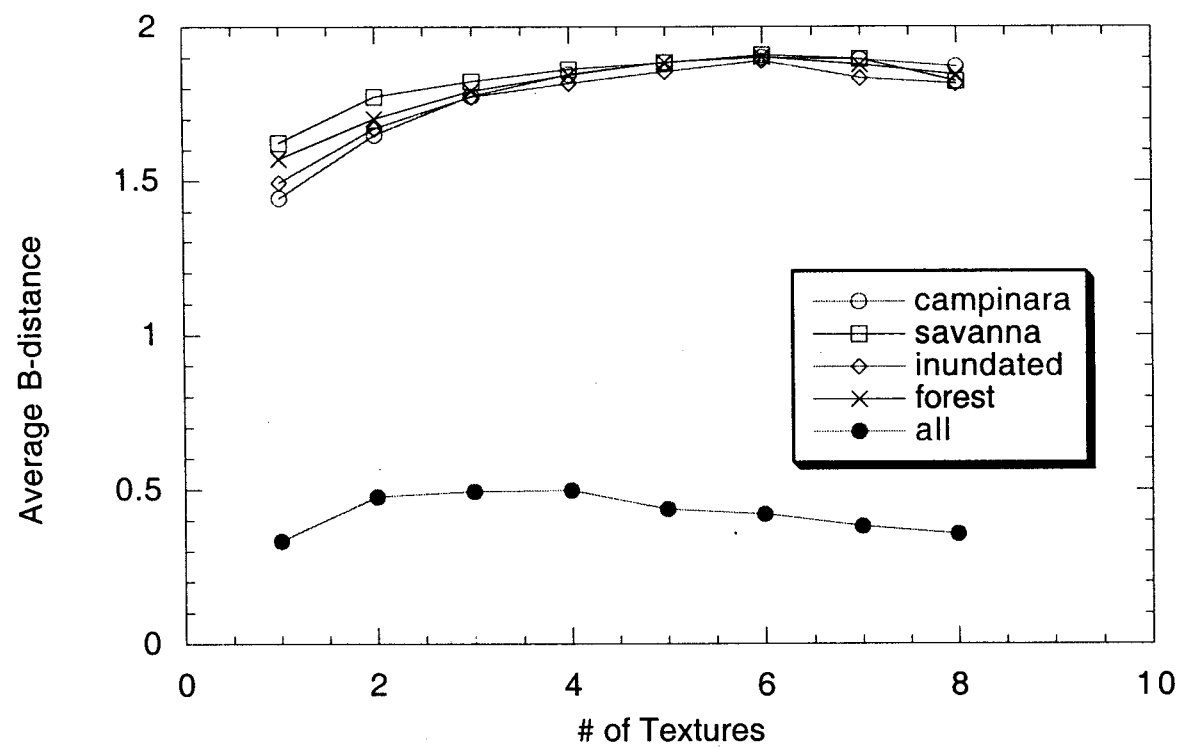
JERS-1 Coverage of Amazon Basin
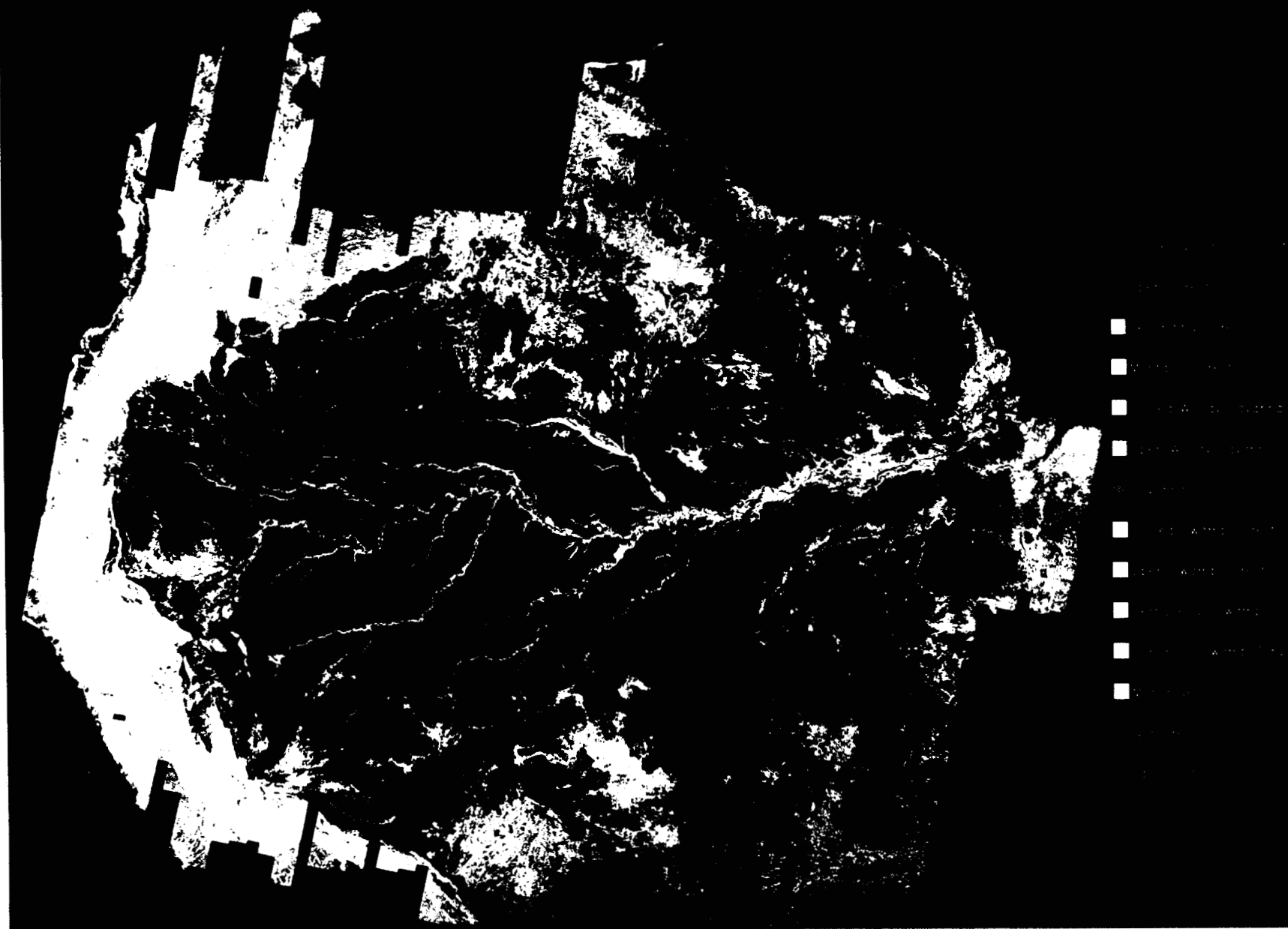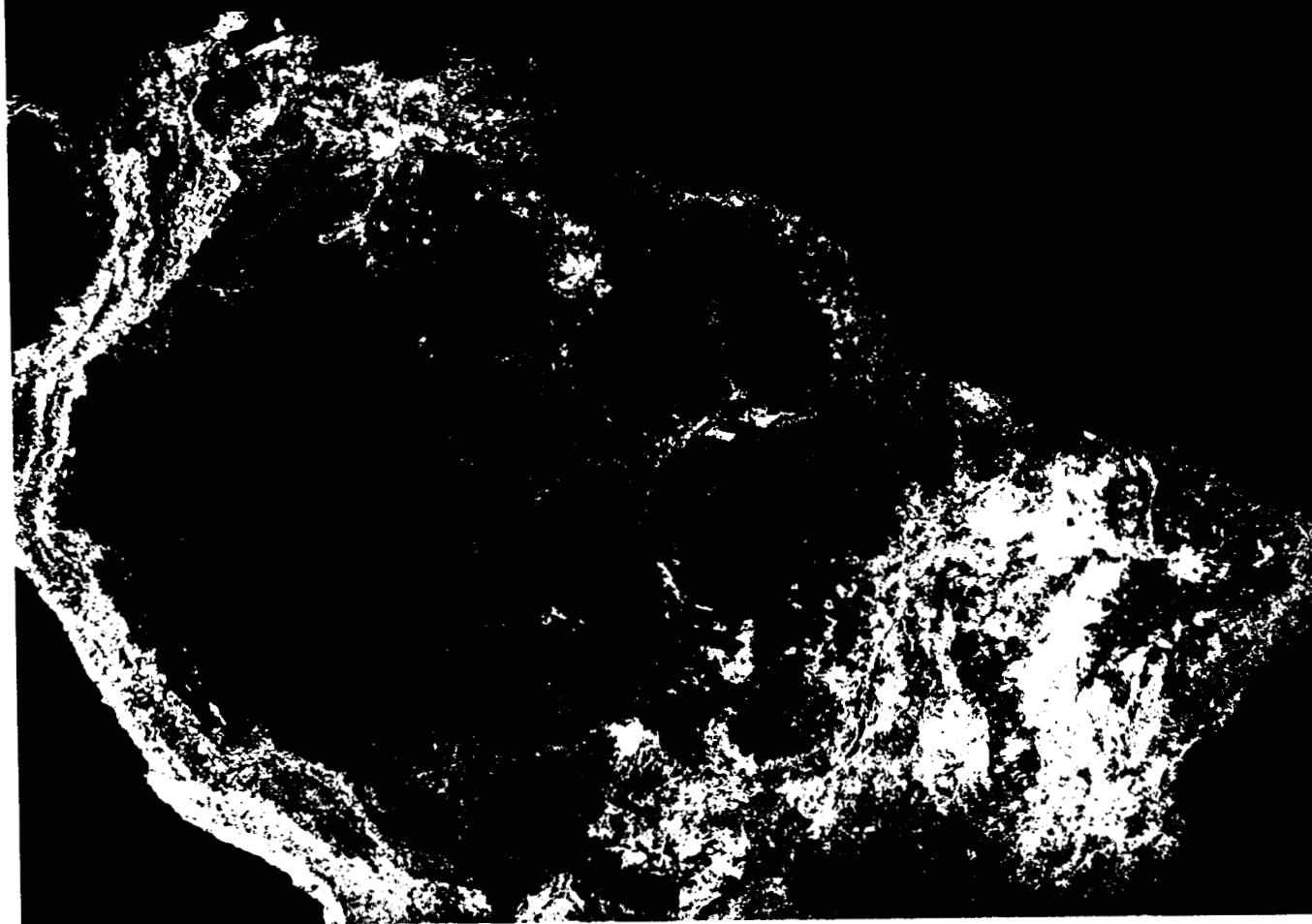
Figure 1.

Vegetation Map of Brazilian Amazon
Scale: 1:2.500.000
IBGE, 1997

Figure 5.

JERS-1 1KM VEGETATION MAP OF AMAZON BASIN
(Saatchi et al., 1998)

AVHRR 1KM LAND COVER CLASSIFICATION
(DeFries et al., 1998)

Evergreen Needleaf Forest

Evergreen Broadleaf Forest

Deciduous Needleaf Forest

Deciduous Broadleaf Forest

Mixed Forest

Closed Shrubland

Open Shrubland

Woody Savanna

Savanna

Grassland

Permanent Wetland

Cropland

Urban

Barren Sparse Vegetated

Open Water